



Influence of the PsbA1/PsbA3, $\text{Ca}^{2+}/\text{Sr}^{2+}$ and Cl^-/Br^- exchanges on the redox potential of the primary quinone Q_A in Photosystem II from *Thermosynechococcus elongatus* as revealed by spectroelectrochemistry

Yuki Kato ^{a,*}, Tadao Shibamoto ^a, Shoichi Yamamoto ^a, Tadashi Watanabe ^a, Naoko Ishida ^b, Miwa Sugiura ^c, Fabrice Rappaport ^d, Alain Boussac ^{b,**}

^a Institute of Industrial Science, University of Tokyo, 4-6-1 Komaba, Meguro-ku, Tokyo 153-8505, Japan

^b iBiTec-S, CNRS UMR 8221, CEA Saclay, 91191 Gif-sur-Yvette, France

^c Cell-Free Science and Technology Research Center, Ehime University, Bunkyo-cho, Matsuyama Ehime, 790-8577, and PRESTO, JST, Honcho, Kawaguchi, Saitama, 332-0012, Japan

^d Institut de Biologie Physico-Chimique, UMR 7141 CNRS-UPMC, 13 rue Pierre et Marie Curie, 75005 Paris, France

ARTICLE INFO

Article history:

Received 16 March 2012

Received in revised form 9 June 2012

Accepted 11 June 2012

Available online 18 June 2012

Keywords:

Photosystem II

Redox potential

Electron transfer

D1 protein

PsbA protein

ABSTRACT

Ca^{2+} and Cl^- ions are essential elements for the oxygen evolution activity of photosystem II (PSII). It has been demonstrated that these ions can be exchanged with Sr^{2+} and Br^- , respectively, and that these ion exchanges modify the kinetics of some electron transfer reactions at the Mn_4Ca cluster level (Ishida *et al.*, *J. Biol. Chem.* 283 (2008) 13330–13340). It has been proposed from thermoluminescence experiments that the kinetic effects arise, at least in part, from a decrease in the free energy level of the Mn_4Ca cluster in the S_3 state though some changes on the acceptor side were also observed. Therefore, in the present work, by using thin-layer cell spectroelectrochemistry, the effects of the $\text{Ca}^{2+}/\text{Sr}^{2+}$ and Cl^-/Br^- exchanges on the redox potential of the primary quinone electron acceptor Q_A , $E_m(\text{Q}_A/\text{Q}_A^-)$, were investigated. Since the previous studies on the $\text{Ca}^{2+}/\text{Sr}^{2+}$ and Cl^-/Br^- exchanges were performed in PsbA3-containing PSII purified from the thermophilic cyanobacterium *Thermosynechococcus elongatus*, we first investigated the influences of the PsbA1/PsbA3 exchange on $E_m(\text{Q}_A/\text{Q}_A^-)$. Here we show that i) the $E_m(\text{Q}_A/\text{Q}_A^-)$ was up-shifted by ca. +38 mV in PsbA3-PSII when compared to PsbA1-PSII and ii) the $\text{Ca}^{2+}/\text{Sr}^{2+}$ exchange up-shifted the $E_m(\text{Q}_A/\text{Q}_A^-)$ by ca. +27 mV, whereas the Cl^-/Br^- exchange hardly influenced $E_m(\text{Q}_A/\text{Q}_A^-)$. On the basis of the results of $E_m(\text{Q}_A/\text{Q}_A^-)$ together with previous thermoluminescence measurements, the ion-exchange effects on the energetics in PSII are discussed.

© 2012 Elsevier B.V. All rights reserved.

1. Introduction

In oxygenic photosynthetic organisms, Photosystem II (PSII), one of the two large pigment–protein complexes, performs the light-driven water oxidation, leading to evolution of proton and dioxygen. The catalytic site for water oxidation is a Mn_4CaO_5 cluster [1], which

Abbreviations: PSII, Photosystem II; Phe *a*, pheophytin *a*, Q_A , primary quinone electron acceptor; Q_B , secondary quinone electron acceptor; Y_Z , redox active tyrosine residue; Chl, chlorophyll; TL, thermoluminescence; SrCl-PSII, $\text{Ca}^{2+}/\text{Sr}^{2+}$ exchanged PSII; CaBr-PSII, Cl^-/Br^- exchanged PSII; CaCl-PSII, untreated PSII; 43H, *T. elongatus* strain with a His-tag on the C terminus of CP43; WT*3, *T. elongatus* strain with a His-tag on the C terminus of CP43 and in which the *psbA1* and *psbA2* genes are deleted; OTTLE, optically transparent thin-layer electrode; DCMU, 3-(3,4-dichlorophenyl)-1, 1-dimethylurea

* Corresponding author at: Present address: Division of Material Science, Graduate School of Science, Nagoya University, Furo-cho, Chikusa-ku, Nagoya, 464-8602, Japan. Tel./fax: +81 52 789 2883.

** Corresponding author.

E-mail addresses: yuki.kato@bio.phys.nagoya-u.ac.jp (Y. Kato), alain.boussac@cea.fr (A. Boussac).

acts as a device accumulating oxidizing equivalents. Light-induced charge separation results in the formation of a radical pair that quickly leads to the formation of the $\text{P680}^+\text{Phe } a^-$ state, where P680 stands for a weakly coupled chlorophyll dimer and Phe *a* for pheophytin *a*. The oxidative power generated with P680^{++} then allows the oxidation of the Mn_4CaO_5 cluster via a redox active tyrosine residue called Y_Z . The oxidation of the Mn_4CaO_5 cluster occurs sequentially forming the S_n states where *n* varies from 0 to 4 [2,3]. Two water molecules are oxidized during the transition from the S_3 state to S_0 via the intermediate S_4 state. Meanwhile, the electron of $\text{Phe } a^-$ is transferred to the plastoquinone pool via the primary and secondary quinone electron acceptors called Q_A and Q_B , respectively.

Ca^{2+} is an essential element for the water oxidation [4,5]. X-ray crystallographic data [1] revealed that Ca^{2+} is linked to all four manganese ions by oxo bridges. In Ca^{2+} depleted PSII the highest oxidation state that can be formed is the S_2Y_Z^* state, and thus water oxidation is inhibited [6,7]. The lost activity can be restored by the addition of Ca^{2+} . Repletion with Sr^{2+} also fully restores the water oxidation mechanism but the oxygen evolution rate of Sr^{2+} -substituted PSII is significantly

lower than that with Ca^{2+} [8,9]. So far Sr^{2+} has been the only divalent cation allowing such substitution and restoration abilities [4,5,8–10].

Cl^- is also indispensable for the turnover of the S-state transitions [4,11]. X-ray crystallographic studies recently identified two Cl^- -binding sites in the vicinity of the cluster and thus suggested that the two anions may contribute to coordination structure of the cluster and also be involved in either proton exit channels or water inlet channels [1,12–14]. Some anions, for example, Br^- , I^- , NO_3^- , and NO_2^- , can substitute for Cl^- [15,16]; a recent study demonstrated that Br^- can support oxygen evolution almost as effectively as Cl^- [13].

The effect of the $\text{Ca}^{2+}/\text{Sr}^{2+}$ and/or Cl^-/Br^- exchange(s) on the oxygen-evolving activity of PSII is reflected by alteration in kinetics and thermodynamics of the S-state transitions. Measurements of time-resolved UV–visible absorption changes and thermoluminescence (TL) revealed that the S_3 to S_0 transition accompanying reduction of Y_Z^+ is significantly slowed down by the ion exchanges, and this slowing down has been rationalized by the decrease in the energy level of S_3 assuming that the ion exchanges affect mainly the electron donor side [17,18]. The $\text{Ca}^{2+}/\text{Sr}^{2+}$ exchange has also been shown to decrease the entropic component in the formation of the transition state in the S_3Y_Z^+ to S_0Y_Z transition [19]. However, it was demonstrated by flash induced fluorescence decay measurements that the $\text{Ca}^{2+}/\text{Sr}^{2+}$ exchange might also decelerate the electron transfer rate from Q_A^- to Q_B [20]. Several studies have shown in addition that Q_A to Q_B electron transfer is influenced by the modification on the donor side of PSII [21,22]. In particular Ca^{2+} depletion has been shown to shift the redox potential of Q_A [23–25]. In the present work, to clarify the $\text{Ca}^{2+}/\text{Sr}^{2+}$ and Cl^-/Br^- exchange effects on the redox properties of the acceptor side, we measured the redox potential of Q_A , $E_m(\text{Q}_A/\text{Q}_A^-)$, in the biosynthetically ion-exchanged PSII complexes from the thermophilic cyanobacterium *Thermosynechococcus elongatus* [17] by using spectroelectrochemistry. This approach has recently proved very powerful as it revealed the spread of the $E_m(\text{Q}_A/\text{Q}_A^-)$ values between species [26,27]. In the light of these results, previous investigations of the redox properties of the Mn_4CaO_5 by TL measurements [17] are also discussed.

Most of the experiments dealing with the biosynthetic ion exchanges were performed in a *T. elongatus* strain in which the *psbA1* and *psbA2* genes, two of the three genes encoding the D1 protein of PSII, had been deleted [28]. Cyanobacteria generally have a *psbA* gene family with 1–6 gene copies (for a review, see Ref. [29]) and *T. elongatus* has three *psbA* genes [30]. *PsbA1* is dominantly expressed under normal growth conditions, whereas *psbA3* is markedly induced under stress conditions such as high light illumination [31–33]. It has also been shown that transcription of *psbA2* is induced by micro-aerobic conditions [34]. The amino acid sequences of these three PsbA proteins are not identical: The processed PsbA1 (344 amino acid residues) differs by 31 and 21 residues from the PsbA2 and PsbA3, respectively. These substitutions cause partially functional differences, particularly in the electron transfer, the water oxidation, and photoprotection [31,33,35–37]. In the present work, to avoid possible complications due to a PsbA exchange when cultivating the cells under abnormal conditions, such as in the presence of Sr^{2+} and Br^- , we used the strain lacking both *psbA1* and *psbA2* [28] and compared the results to those obtained with PsbA1-PSII.

2. Materials and methods

Biosynthetically $\text{Ca}^{2+}/\text{Sr}^{2+}$ or Cl^-/Br^- exchanged PSII (hereafter, SrCl-PSII and CaBr-PSII) as well as untreated PSII (CaCl-PSII) complexes were isolated, as described previously [17], from a *T. elongatus* WT*3 strain [28], which is a His-tagged CP43 strain (43-H) [38] with genetic modification to possess only the *psbA3* gene. The WT*3 cells were cultured in a DTN medium containing 0.8 mM CaCl_2 ; for the isolation of SrCl-PSII or CaBr-PSII, the culture medium was supplemented with 0.8 mM SrCl_2 or CaBr_2 , respectively, instead of CaCl_2 [17]. Oxygen-

evolving activities of the purified PSII complexes were 5000–6000, 1800–2600, and 3200–3600 $\mu\text{mol O}_2 \text{ mg Chl}^{-1} \text{ h}^{-1}$ for CaCl-PSII, SrCl-PSII, and CaBr-PSII, respectively [17]. The purified PSII complexes were stored in liquid nitrogen at a concentration of about 1.5–2.0 mg Chl mL^{-1} in a medium containing 10% glycerol, 1 M betaine, 40 mM MES-NaOH (pH 6.5), 15 mM CaCl_2 and 15 mM MgCl_2 (instead, CaBr_2 and MgBr_2 for CaBr-PSII), until they were used.

Spectroelectrochemical measurements have been carried out in essentially the same manner as in previous work [26]. The PS II samples were suspended at a Chl *a* concentration of 150 μM , corresponding to 4.3 $\mu\text{M Q}_A$, in a medium containing 50 mM MES-NaOH (pH 6.5), 0.1% dodecyl- β -D-maltoside, 1 M glycine-betaine, 1% taurine, 15 mM CaCl_2 , 15 mM MgCl_2 , and 200 mM KCl; for CaBr-PSII, CaBr_2 , MgBr_2 and KBr were used instead. A combination of the following redox mediators were added into the medium: 50 μM anthraquinone-2-sulfonate ($E_m = -195 \text{ mV}$), 50 μM 2-hydroxy-1,4-naphthoquinone ($E_m = -100 \text{ mV}$) and 100 μM *N,N,N',N'*-tetramethyl-*p*-phenylenediamine ($E_m = +300 \text{ mV}$). A sample solution was transferred into an optically transparent thin-layer electrode (OTTLE) cell equipped with a gold mesh (100 mesh/inch) working electrode, a Pt black counter electrode and a Ag–AgCl reference electrode [39]. The electrode potential was controlled with a potentiostat Model 2020 (Toho Technical Research). The electrode potential is hereafter referred to the standard hydrogen electrode SHE (0 mV vs. Ag–AgCl is equivalent to +199 mV vs. SHE). The Chl fluorescence was excited with a weak monochromatic beam of 430 nm light, and the emission in line with the measuring beam was detected at the backside of the OTTLE cell placed in a sample chamber of a spectrofluorometer (FP6500/JASCO). The spectroelectrochemical measurements were performed at 14 °C. For the measurements of the ratio of fluorescence maximum level to minimum one (F_m/F_0) of the PSII sample solutions, a double-modulation fluorometer model FL-3500 (Photon Systems Instruments) was used.

3. Results

3.1. Redox potential of Q_A in CaCl-PSII with *PsbA3* as the D1 protein (PsbA3-PSII)

Previous spectroelectrochemical measurements have been performed with PsbA1-PSII [26]. Even though exchanging D1 encoded by *psbA1* for that encoded by *psbA3* is not expected to significantly alter the properties of Q_A since it is bound by D_2 , TL and temperature dependence of the fluorescence decay performed on both PSII suggested that the $E_m(\text{Q}_A/\text{Q}_A^-)$ might differ [35]. We thus first characterized the CaCl-PSII purified from WT*3 (CaCl-PsbA3-PSII).

Fig. 1A shows the evolution of the fluorescence intensity at 681 nm resulting from stepwise potential changes. As shown in Ref. [26] this wavelength corresponds to the peak of the fluorescence emission spectrum and its intensity reflects the redox state of Q_A . To allow the comparison of these spectroelectrochemical results with the previous ones [26], we avoided freeze-thawing that has been shown to induce a shift in the $E_m(\text{Q}_A/\text{Q}_A^-)$ value [24], i.e., after purification the PsbA3-PSII samples were kept at 4 °C until use. Assuming that the fluorescence change resulting from electrochemical reduction is proportional to the fraction of Q_A reduced to Q_A^- , Nernstian plots were constructed for the magnitude of the fluorescence intensity against the electrode potential (Fig. 1B, see also Fig. S1, Supplementary Material). The data obtained for PsbA3-PSII are nicely fitted with a theoretical one-electron redox process, and three independent measurements yielded a value of $-102 \pm 2 \text{ mV}$ for $E_m(\text{Q}_A/\text{Q}_A^-)$ in PsbA3-PSII. This is 38 mV more positive than the previous value obtained for $E_m(\text{Q}_A/\text{Q}_A^-)$ in PsbA1-PSII ($-140 \pm 2 \text{ mV}$, Ref. [26]). Even considering possible deviations for a linear relationship between the fluorescence yield and the redox state of Q_A [27,40], which can be estimated on the basis of the F_m/F_0 values (3.7 and 5.9

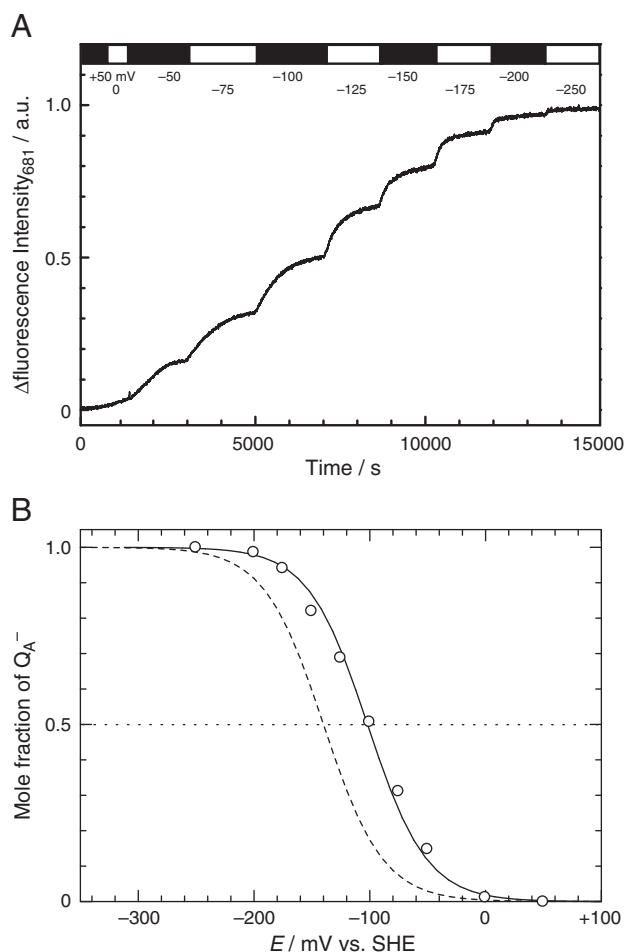


Fig. 1. Spectroelectrochemical outcome from redox reaction of Q_A in PsaA3-PSII isolated from *T. elongatus*: (A) Fluorescence intensity change at 681 nm during a potential journey from +50 mV to –250 mV for the PSII complexes; (B) Nernstian plot based on the relative values of the fluorescence intensity. The solid curve in (B) represents a theoretical one for one-electron redox process with $E_m = -102$ mV; the dashed curve is drawn for a theoretical one-electron redox process with $E_m = -140$ mV, which is the result for PsaA1-PSII from *T. elongatus* (cf. Ref. [26]). For the measurements, PSII samples without freeze-thawing were used.

for PsaA1-PSII and PsaA3-PSII, leading to the deviations of 16 and 19 mV, respectively; see Table 1), the difference in the $E_m(Q_A/Q_A^-)$ values found here can be considered as significant.

Spectroelectrochemical measurements of $E_m(\text{Phe } a/\text{Phe } a^-)$ for both PSII [35,41] previously revealed that the $E_m(\text{Phe } a/\text{Phe } a^-)$ value of PsaA3-PSII is 17 mV more positive than that of PsaA1-PSII

Table 1
Redox potential values of Q_A/Q_A^- and experimental parameters for PSII complexes from *T. elongatus*.

PSII	$E_m(\text{exp})^a/\text{mV vs. SHE}$	$E_m(R=1)^b/\text{mV vs. SHE}$	$R (F_m/F_0)$
PsaA3-PSII	-102 ± 2	-83 ± 2	5.9
PsaA1-PSII ^c	-140 ± 2	-124 ± 2	3.7

^a Experimental values determined by spectroelectrochemistry: The value for PsaA3-PSII is an average of three independent measurements; the value for PsaA1-PSII is an average of four independent measurements [26]. For the measurements, PSII samples without freeze-thawing were used.

^b “True” values estimated from $E_m(\text{exp})$ by considering possible deviation from a linear relationship between the fluorescence yield and the redox state of Q_A . The deviations can be estimated on the basis of values of F_m/F_0 (cf. [27,40]).

^c The values cited from the previous work [26,27].

(-522 ± 3 mV and -505 ± 6 mV for PsaA1-PSII and PsaA3-PSII, respectively). This difference in the redox potential can be ascribed to the difference in the amino acid residue at position 130 of PsaA (D1–130), which is located at a hydrogen bond distance from the 13¹-keto C=O group of Phe *a* [1]: The residue in PsaA1 is a Gln and a Glu in PsaA3. A recent FTIR study together with theoretical calculations [42] showed that the Glu side-chain expectedly provides a stronger hydrogen bond to the 13¹-keto C=O group of Phe *a*[−] anion, leading to a more positive value of $E_m(\text{Phe } a/\text{Phe } a^-)$. As regards to redox potentials, the difference between PsaA1-PSII and PsaA3-PSII is larger for Q_A than for Phe *a* and, even more importantly, these respective shifts in E_m result in an increase in the absolute of ΔE_m , rather than a decrease as would be expected from the stabilization of Phe *a*[−] by the D1–Q130E substitution.

Before the development of the spectroelectrochemical measurements described earlier [26] and here, which provide means to assess the redox potentials of the cofactors of interest, TL measurements have been performed to investigate the effects of the PsaA1 to PsaA3 substitution on the energetics [31,33,35]. Outcomes of TL, namely peak temperature and intensity of an emission band, depend on the free energy gaps between the excited state of P680 (P680*) and the charge separated states, [P680⁺⁺ Phe *a*[−]], S₂Q_A[−] or S₂Q_B[−] [43,44]. Though TL data thus reflect total changes in free energy gaps (\approx redox potential differences) of these cofactors, one can refer to site-directed mutagenesis studies on this position in *Synechocystis* sp. PCC 6803, as a model case concerning the D1–Q130E substitution, that demonstrated the relationship between the shift of $E_m(\text{Phe } a/\text{Phe } a^-)$ and the TL data changes [45–47]: Time resolved absorption measurements lead to an estimation of +33 mV [46] up-shift for the $E_m(\text{Phe } a/\text{Phe } a^-)$ resulting from the D1–Q130E substitution, and on the other hand, +30–38 mV [47] was calculated from a change in TL intensity. Further, the theoretical effects of the $E_m(\text{Phe } a/\text{Phe } a^-)$ shift on the TL data were satisfyingly simulated in terms of intensities and peak temperatures [44]. A lower intensity in the TL B-band together with a small down-shift of the peak temperature has also been reported in *T. elongatus* whole cells containing PsaA3-PSII induced by cultivation under strong light illuminations [31] instead of PsaA1-PSII and in deletion mutants with only the *psbA₃* gene when compared to a deletion mutant with only the *psbA₁* and *psbA₂* genes [33]. These variations were similar to those observed in *Synechocystis* 6803 but their extent of the difference in *T. elongatus* was smaller, suggesting a +18–20 mV shift of $E_m(\text{Phe } a/\text{Phe } a^-)$; this was explained by the compensatory effects of some of the substituted amino acid residues between PsaA1 and PsaA3 other than D1–Q130E, such as D1–Leu151Val and D1–Ser124Phe, being located in the vicinity of the Phe *a*. On the other hand, TL measurements made on PsaA1-PSII and PsaA3-PSII complexes isolated from *T. elongatus* yielded contradictory results to those obtained with the *T. elongatus* cells [33,35]: The peak intensity obtained with PsaA3-PSII was found larger while the peak temperature was similar for both PSII. These results are inconsistent with the idea that only the $E_m(\text{Phe } a/\text{Phe } a^-)$ would be shifted. In view of this, the unexpected shift of $E_m(Q_A/Q_A^-)$ found in the present work might contribute to the contradictory TL results. Hence we attempted to analyze the TL data of the two types of PSII [35] on the basis of the recent theory [44] applied with their $E_m(\text{Phe } a/\text{Phe } a^-)$ and $E_m(Q_A/Q_A^-)$ shifts (See Fig. S2, Supplementary Material).

A simulation assuming only the $E_m(\text{Phe } a/\text{Phe } a^-)$ shift by +17 mV indicates that the peak temperature of the TL band should be lower and the intensity should be smaller (green-solid curve in Fig. S2) when compared with the control, namely PsaA1-PSII (black-solid curve); this assumption reproduces qualitatively the result obtained from the site-directed mutation of the D1–Q130E in *Synechocystis* 6803 [47]. Meanwhile, assuming the $E_m(\text{Phe } a/\text{Phe } a^-)$ and $E_m(Q_A/Q_A^-)$ are shifted by +17 mV and +40 mV, respectively, simulations show that the peak temperature and intensity should be higher and smaller, respectively (blue-solid curve), at variance with experimental results for the PsaA1-PSII and PsaA3-PSII complexes [35]. As a

consequence, though the TL data cannot be rationalized even with the $E_m(\text{Phe } a/\text{Phe } a^-)$ and $E_m(\text{Q}_A/\text{Q}_A^-)$ shifts, the latter shift, reported here, might contribute partly to the almost similar peak temperature observed in the TL experimental curves.

3.2. Biosynthetic $\text{Ca}^{2+}/\text{Sr}^{2+}$ or Cl^-/Br^- exchange influences on the redox potential of Q_A in PSII composed of PsbA3

As shown in Ref. [17,18], *T. elongatus* cells can be photoautotrophically grown in Sr^{2+} -containing media instead of Ca^{2+} and also in Br^- -containing media instead of Cl^- , resulting in the biosynthetically ion-exchanged PSII complexes, SrCl-PSII and CaBr-PSII. A previous study showed that the substituted Sr^{2+} in the Mn_4 -cluster ion is not spontaneously exchangeable for Ca^{2+} ions in Ca^{2+} -containing media [18]; on the other hand, the exchange of Br^- for Cl^- in the Cl^- -binding sites occurs [12,13,17]. Therefore, the spectroelectrochemical measurements for CaCl-PSII and SrCl-PSII were performed with solutions containing Cl-salts as electrolyte, and CaBr-PSII were studied with solution containing Br-salts.

Fig. 2 shows the Nernstian curves for the redox reaction of Q_A based on the spectroelectrochemical outcomes, as obtained as Fig. 1A (see also Supplementary Material, Figs. S3–S5A), for the three types of PSII, i.e., CaCl-PSII, CaBr-PSII and SrCl-PSII all composed of PsbA3. Since measurements on CaBr-PSII and SrCl-PSII were done with once-frozen samples we have also determined the redox potential of Q_A in a once-frozen CaCl-PSII sample. The three sets of data could be satisfyingly fit by a one-electron theoretical Nernstian curve. However, as shown in Figs. S3–S5B (Supplementary Material), the slopes of data sets in a semi-logarithmic plot were 67–71 mV per decade, i.e., larger than the theoretical value of 57 mV at 14 °C. In contrast, the slopes of the data points for the non-exchanged PsaB3-PSII (CaCl-PSII) samples without freeze-thawing (Fig. S1) were 55 ± 3 mV per decade (58 ± 3 mV per decade for PsaB1-PSII [26]), i.e., close to the theoretical value. This suggests that the deviations from the Nernst equation might stem from freeze-thawing that would induce heterogeneity in the sample and yield a less negative $E_m(\text{Q}_A/\text{Q}_A^-)$ value of -89 ± 2 mV for CaCl-PSII than -102 ± 2 mV for the non-frozen samples.

Krieger and co-workers [24] reported that freezing and thawing of oxygen-evolving PSII samples at low potentials where Q_A is reduced induces an irreversible change in the $E_m(\text{Q}_A/\text{Q}_A^-)$ value to over 150 mV more positive values owing to structural perturbation at the donor side of PSII. The rather small redox potential difference

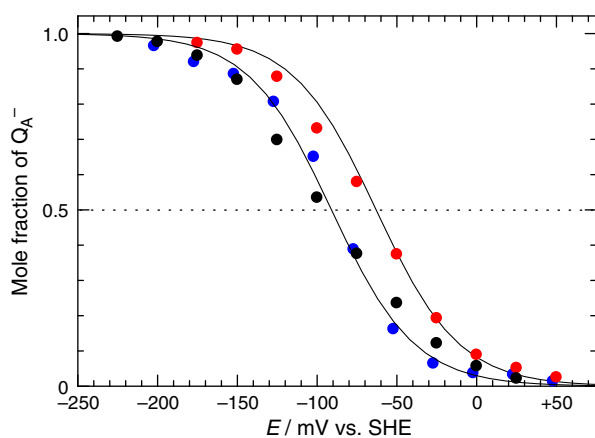


Fig. 2. Nernstian plot for the redox reaction of Q_A in the PSII complexes based on the relative values of fluorescence intensity at 681 nm; for CaCl-PSII (black), CaBr (blue), SrCl (red). The lines represent a theoretical one for a one-electron redox process with $E_m = -62$ mV or -89 mV.

(13 mV) reported here shows that in the present case with PSII from *T. elongatus* the freezing-induced shift here is not so influential.

In once-frozen samples, i.e., with samples comparable to those used in all the previous spectroscopic studies, the results clearly indicate that the $E_m(\text{Q}_A/\text{Q}_A^-)$ value of -88 mV for CaBr-PSII is almost the same as that for CaCl-PSII (-89 mV), whereas the $E_m(\text{Q}_A/\text{Q}_A^-)$ value for SrCl-PSII (-62 mV) is 27 mV more positive, as summarized in Table 2. We did not find any significant difference for the $E_m(\text{Q}_A/\text{Q}_A^-)$ when measured in the presence of Br⁻ salts rather than Cl⁻ salts (data not shown). The difference in the $E_m(\text{Q}_A/\text{Q}_A^-)$ values between CaCl-PSII and SrCl-PSII is significant even in light of deviations for the linear relationship between the fluorescence yield and the redox state of Q_A (see Table 2). It can thus be concluded that modification in the Ca^{2+} -binding site, but not in the Cl^- -binding site, influences on $E_m(\text{Q}_A/\text{Q}_A^-)$.

4. Discussion

We report here that the $\text{Ca}^{2+}/\text{Sr}^{2+}$ exchange at the Mn_4CaO_5 cluster of PsaB3-PSII from *T. elongatus* up-shifts $E_m(\text{Q}_A/\text{Q}_A^-)$ by ca. 27 mV. This is at variance with Cl^-/Br^- exchange that hardly influences $E_m(\text{Q}_A/\text{Q}_A^-)$. As mentioned in the Introduction, the effects of the $\text{Ca}^{2+}/\text{Sr}^{2+}$ and/or Cl^-/Br^- exchange(s) on the oxygen-evolving activity of PSII have been observed by many authors. More precisely, it has been proposed that the $\text{Ca}^{2+}/\text{Sr}^{2+}$ exchange affects the redox properties of the oxygen-evolving Mn_4CaO_5 cluster because of the difference in physico-chemical properties like the atomic radius and Lewis acidity of the two cations, as suggested by EPR [18,48], FTIR [49–51], EXAFS spectroscopy [52,53] and so on. There are in addition several pieces of evidences pointing to effects of the ion exchange on the thermodynamics and kinetic properties of Q_A and/or Q_B . Kargul et al. demonstrated, on the basis of the flash induced fluorescence decay measurements [20], that the $\text{Ca}^{2+}/\text{Sr}^{2+}$ exchange induces a slowing down of the Q_A to Q_B electron transfer. Further, an EPR study [48] showed that the $\text{Ca}^{2+}/\text{Sr}^{2+}$ exchange possibly induces slight change in the environment of the non-heme iron located between Q_A and Q_B . Saliently, removal of the Mn and/or Ca ions from PSII induces a ca. 150 mV positive shift of $E_m(\text{Q}_A/\text{Q}_A^-)$ [23–25]. The structural rationales behind these long distance effect remains to be identified, but a likely hypothesis is that the membrane spanning helices mediate the structural change [23]. In view of these studies and the present result, it can be proposed that the $\text{Ca}^{2+}/\text{Sr}^{2+}$ exchange probably induces slight structural change on the stromal (cytoplasmic) side. Yet, the extent of these changes is presumably smaller than that induced by the removal of Ca^{2+} , and so is the resulting shift of $E_m(\text{Q}_A/\text{Q}_A^-)$ (+27 mV instead of +150 mV). As regards to Cl^- , Cl^- -depletion hardly affects $E_m(\text{Q}_A/\text{Q}_A^-)$ [25]. Consistent with this, we did not find any change in $E_m(\text{Q}_A/\text{Q}_A^-)$ upon Cl^-/Br^- exchange.

The consequences of the $\text{Ca}^{2+}/\text{Sr}^{2+}$ or Cl^-/Br^- exchange on the overall energetics of PSII have been previously discussed on the basis

Table 2

Redox potential values of Q_A/Q_A^- and experimental parameters for CaCl-PSII (PsaB3-PSII), $\text{Ca}^{2+}/\text{Sr}^{2+}$ or Cl^-/Br^- biosynthetically exchanged PSII complexes.

PSII	$E_m(\text{exp})^a/\text{mV}$ vs. SHE	$E_m(R=1)^b/\text{mV}$ vs. SHE	$R (F_m/F_0)$	TL in S_2Q_B^c
SrCl	-62	-44	5.7	52
CaBr	-88	-69	6.0	50
CaCl	-89	-70	5.9	48

^a Experimental values obtained by spectroelectrochemistry: The value for SrCl-PSII is an average of two independent measurements, -65 mV and -58 mV; the value for CaBr-PSII is an average of three independent measurements with a S.D. of ± 2 mV; the value for CaCl-PSII is an average of three independent measurements with a S.D. of ± 2 mV.

^b "True" values estimated from $E_m(\text{exp})$ by considering possible deviation from a linear relationship between the fluorescence yield and the redox state of Q_A . The deviations can be estimated on the basis of values of F_m/F_0 (cf. [27,40]).

^c Temperature peak position of the thermoluminescence glow curves from the S_2Q_B charge recombination; the values cited from Ref. [17].

of TL data [17]. However, the here-reported shift of the $E_m(Q_A/Q_A^-)$ upon Ca^{2+} to Sr^{2+} exchange was not known at this time and hence not taken into account. This issue thus needs revision in the light of the present results. According to literature data, the redox potential difference between the Q_A and Q_B acceptors in isolated thylakoids is ca. 70 mV [54,55]. Under comparable conditions the temperature difference between the corresponding Q and B TL bands is ca. 20 °C [55]. As regards to the donor side, it has been shown in [17] that, in *T. elongatus* PSII, the TL arising from the $S_3Q_B^-$ is shifted by 6 °C with respect to that of $S_2Q_B^-$, a shift with should reflect the 20 meV increase in energy level of S_3 with respect to S_2 (for a review, see Ref. [56]). These figures lead to an empirical relationship of 0.3–0.4 K meV⁻¹ (for a recent review on this issue, see Ref. [44]). On the basis of these estimates and of the here-reported shift of the $E_m(Q_A/Q_A^-)$ one can attempt to draw an accurate picture of the energetic consequences of the Ca^{2+} to Sr^{2+} exchange. The TL peak temperature for the $S_2Q_B^-$ charge recombination has been shown to be up-shifted by ≈ 2 °C upon the Ca^{2+}/Sr^{2+} exchange [17]. Since the redox properties of the Mn_4 cluster in the S_2 state were not modified by this exchange [18] it seems likely that the up-shift by ≈ 2 °C results from the contribution of the increase in the $E_m(Q_A/Q_A^-)$ value in the $S_2Q_B^-$ charge recombination. Expectedly, this 2 °C shift is smaller than expected if one applies the 0.3–0.4 K meV⁻¹ coefficient to the 27 mV shift in redox potential because what mostly determines the TL curve in this case is the free energy gap between Q_B^- and $Phe a^-$.

It has been shown that the Ca^{2+}/Sr^{2+} exchange induces a decrease in the energy level of the S_3 state [17]. In addition it induces an up-shift of the TL peak by ≈ 4 °C [17]. Taking into account the 2 °C originating from the contribution of the $E_m(Q_A/Q_A^-)$ the remaining 2 °C likely reflects the decrease in the energy levels of the S_3 state in SrCl-PSII when compared to CaCl-PSII. Applying the 0.3–0.4 K meV⁻¹ coefficient, this translates into a ≈ 5 –7 mV up-shift in the redox potential of the S_3/S_2 couple in the SrCl-PSII compared to CaCl-PSII. As a consequence,

the Ca^{2+}/Sr^{2+} or Cl^-/Br^- exchange effects on the energetics in PSII are summarized in Fig. 3. In Ca^{2+}/Sr^{2+} and also Cl^-/Br^- exchanged PSII complexes (SrBr-PSII), the shift of the peak temperature of the TL curve resulting from the $S_3Q_B^-$ charge recombination is 6 °C [17], which, following the same reasoning as above, translates into a $(6 - 2)/0.3 - 0.4 = 10$ –14 mV shift of the S_3/S_2 couple redox potential resulting from the CaCl to SrBr substitution. In relation to the result of Kargul et al. [20], our results also suggest that the deceleration of the electron transfer rate between Q_A and Q_B induced by the Ca^{2+}/Sr^{2+} exchange might stem from the decrease in the free energy change of the electron transfer, the extent of which should correspond to the $E_m(Q_A/Q_A^-)$ difference in the two types of PSII.

We also found out that the $E_m(Q_A/Q_A^-)$ value of PsbA3-PSII is ca. 40 mV more positive than that of PsbA1-PSII which is dominantly expressed under usual growth conditions for *T. elongatus* (Fig. 1 and Table 1). At first sight, this shift in $E_m(Q_A/Q_A^-)$ may seem unexpected because Q_A is bound to PsbD (D2) rather than PsbA (D1). However, Q_A is linked to the Q_B binding site, made by the D1 protein, through the Q_A -His214(D2)-Fe-His215(D1)- Q_B molecular bridge. A FTIR study together with docking calculations [57] suggested that the hydrogen bond strength between D1-His215 and Q_B influences the hydrogen bond strength between D2-His214 and Q_A through this molecular bridge, so that any change in the Q_B site may propagate through this H-bond wire to Q_A and possibly lead to a shift of $E_m(Q_A/Q_A^-)$. Notably, switching from PsbA1 to PsbA3 results in an amino acid substitution at position 270 (Ser in PsbA1, Ala in PsbA3) [31], which might modify the structure of the Q_B site by changing the hydrogen bond strength with D1-His215, and hence shift $E_m(Q_A/Q_A^-)$. As mentioned in [35], D1-S270A substitution may also contribute to loosen the hydrogen bond with the head group of a lipid sulfoquinovosyldiacylglycerol (SQDG) located in the Q_B site and may be the rationale behind the difference of the binding characteristics of herbicides such as DCMU or bromoxynil to the Q_B site. In addition, an EPR study [58] indicated that

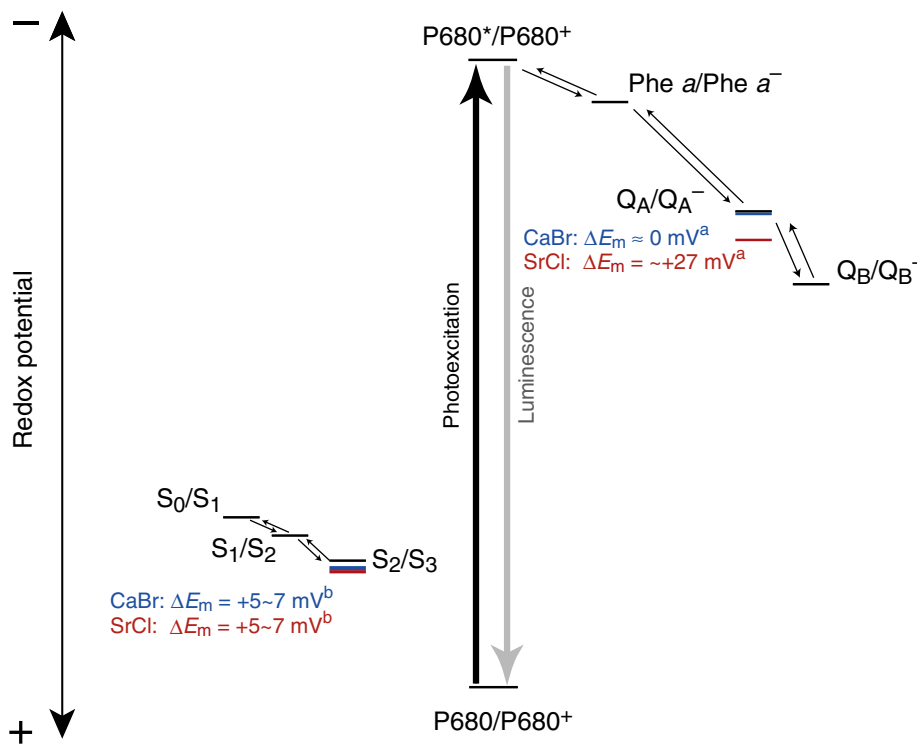


Fig. 3. Schematic diagram for the ground and charge separated states in PSII based on the redox potentials: (a) The differences in the $E_m(Q_A/Q_A^-)$ values between CaCl-PSII (PsbA3-PSII) and biosynthetically ion-exchanged PSII, SrCl-PSII or CaBr-PSII, were determined by the spectroelectrochemical measurements in the present work; (b) Taking into account a part of the peak temperature difference of the thermoluminescence glow curves for $S_3Q_B^-$ charge recombination [17] originating from the contribution of the $E_m(Q_A/Q_A^-)$ shift, the difference in the $E_m(S_2/S_3)$ values is estimated empirically (for detail, see text).

E_m of the non-heme iron, which is a link in the molecular bridge, is more positive in PsbA1-PSII than in PsbA3-PSII.

It is remarkable that the difference in $E_m(Q_A/Q_A^-)$ (ca. 40 mV) between PsbA1-PSII and PsbA3-PSII is larger than that of $E_m(\text{Phe } a/\text{Phe } a^-)$ (17 mV) which is directly, within a hydrogen bond distance, linked to the D1-Q130E substitution. In *T. elongatus*, the PsbA3 (D1) protein that differ by 21 amino acids from PsbA1 is expressed under high light conditions [26,33], and hence this PsbA substitution has been proposed to contribute to photoprotection [33,35,37,42]. Indeed, PSII can undergo photo-damage and this is considered to originate, at least in part, from the production of harmful $^1\text{O}_2$ accompanying the decay of $^3\text{P680}$ (for reviews, see Refs. [59–61]). The critical parameter is thus whether or not $^3\text{P680}$ is formed during charge recombination. It has been pointed out that the decrease in the energy gap between $\text{Pheo}_{D1}^+\text{Q}_A$ and $\text{Pheo}_{D1}\text{Q}_A^-$ in PsbA3-PSII resulting from the shift in $E_m(\text{Phe } a/\text{Phe } a^-)$ induced by the D1-Q130E substitution would make the repopulation of the $\text{Pheo}_{D1}^+\text{Q}_A$ state easier in PsbA3-PSII than in PsbA1-PSII [59] and thus disfavor the direct charge recombination between P680^{++} and Q_A^- . Since formation of $^3\text{P680}$ involves the formation of the $^3[\text{P680}^{++}\text{Pheo}_{D1}^-]$, this paradoxically would imply that PsbA3-PSII would be more prone to photo-damage than PsbA1-PSII. To get round this contradiction, it has been proposed that owing to its very large driving force (~ 1.6 eV), the charge recombination from $^1[\text{P680}^{++}\text{Pheo}_{D1}^-]$ to P680Pheo_{D1} operates in the inverted region of the Marcus curve where the rate of the electron transfer reactions increases when the driving force decreases [59]. This means that the charge recombination from $^1[\text{P680}^{++}\text{Pheo}_{D1}^-]$ (to the detriment of the population of the $^3[\text{P680}^{++}\text{Pheo}_{D1}^-]$ state) would be faster in PsbA3-PSII than in PsbA1-PSII. Further, Rutherford et al. [61] recently proposed that the expected accumulated state under high light conditions is $\text{Pheo}_{D1}\text{Q}_A^-$ rather than $\text{Pheo}_{D1}\text{Q}_A^-$ so that the energy gap between the $\text{Pheo}_{D1}\text{Q}_A^-$ and $\text{Pheo}_{D1}^+\text{Q}_A$ states would not be the most relevant parameter and that the tuning of the respective yield of the various recombination pathway would reside in the $^1[\text{P680}^{++}\text{Pheo}_{D1}^-]$ to P680Pheo_{D1} charge recombination. In any case the here-reported 40 mV up-shift of the $E_m(Q_A/Q_A^-)$ associated with the switch from PsbA1-PSII to PsbA3-PSII is an additional parameter that needs being taken into account. This up-shift results in a larger free energy gap between $\text{Pheo}_{D1}\text{Q}_A^-$ and $\text{Pheo}_{D1}^+\text{Q}_A$ and this will contribute to prevent the formation of the $^3[\text{P680}^{++}\text{Pheo}_{D1}^-]$ state under light conditions that do not yield the accumulation of $\text{Pheo}_{D1}^+\text{Q}_A^-$. In addition, the lower energy level of $\text{P680}^{++}\text{Phe } a^-$, resulting from the more positive $E_m(\text{Phe } a/\text{Phe } a^-)$, should increase the quantum yield of PSII as shown in the case of site-directed mutants [45,46,62]. Consistent with this, we found a larger $(F_m - F_0)/F_m$ ratio in PsbA3-PSII than in PsbA1-PSII (0.83 versus 0.73; cf. Table 1). Yet, we acknowledge the fact that the rationale for increasing the quantum yield under high, i.e. non limiting light intensity is not obvious. This may not be a functional requirement but merely the consequence of the fine tuning required to minimize $^3\text{P680}$ formation. In conclusion, in *T. elongatus*, PsbA3 has many reasons to be preferentially expressed under high light conditions, while it should remain to be cleared whether photoprotection induced by PsbA substitution accompanying the $E_m(Q_A/Q_A^-)$ shift as shown here for *T. elongatus* may be generalized to other cyanobacteria or not.

In light of the discrepancy between the TL experimental results and the simulation based on the $E_m(\text{Phe } a/\text{Phe } a^-)$ and $E_m(Q_A/Q_A^-)$ shifts (Fig. S2), the redox properties of the other redox cofactors might be modified; as pointed out previously [35], the TL intensity also reflects fraction of PSII with Q_B^- in the dark, these centers being silent after one flash in TL experiment. Moreover, the addition of DCMU to PSII centers with Q_B^- shifts to the right the equilibrium of $\text{Q}_A\text{Fe}^{\text{II}}\text{Q}_B^- \leftrightarrow \text{Q}_A^-\text{Fe}^{\text{II}}\text{Q}_B$ [58,63,64] resulting in closed reaction centers. An EPR study [58] also demonstrated that upon the addition of DCMU the shift of $\text{Q}_A\text{Fe}^{\text{II}}\text{Q}_B^-$ toward $\text{Q}_A\text{Fe}^{\text{III}}\text{Q}_B\text{H}_2$, silent in TL, also occurred in PsbA3-PSII but not in PsbA1-PSII. These multiple modifications of the redox cofactors as well as the revealed differences in $E_m(\text{Phe } a/\text{Phe } a^-)$ and in $E_m(Q_A/Q_A^-)$

likely explain the TL experimental results for the two types of PSII and also contribute to the higher quantum yield.

In any case, the present findings show that the tuning of the redox potentials of cofactors involved in PSII function is exquisitely subtle. Slight structural modifications at the donor side may affect the redox potential of a quinone located more than 25 Å apart and shifting from PsbA3 to PsbA1 have multiple functional consequences. This likely illustrates the necessary shaping, imposed by the oxygen rich environment, of the relative yield of forward and productive reactions, on the one hand, and of the energy wasting ones on the other hand [61]. From a more general stand point, it shows that the rationale behind the gene regulation that control the expression of the *psbA3* and *psbA1* genes in response to different light regimes does not sum up to the effect of a single amino acid substitution and that further studies, including X-ray approaches, will be required to fully understand the physiological significance of this regulation.

Acknowledgements

We thank Dr. H. Wada and Dr. N. Mizusawa for letting us use a double-modulation fluorometer FL3500. This work was supported in part by a Grant-in-Aid for Scientific Research (Nos. 21750012 to Y.K., 22550146 to T.W., and 21612007 to M.S.) from the Japan Society for the Promotion of Science (JSPS), a global COE program for “Chemistry Innovation through Cooperation of Science and Engineering” (to T.S. and T.W.) from the Ministry of Education, Culture, Sports, Science and Technology (MEXT), and a JST-PRESTO program (4018 to M.S.).

Appendix A. Supplementary data

Supplementary data to this article can be found online at <http://dx.doi.org/10.1016/j.bbabi.2012.06.006>.

References

- Y. Umena, K. Kawakami, J.-R. Shen, N. Kamiya, Crystal structure of oxygen-evolving photosystem II at a resolution of 1.9 Å, *Nature* 473 (2011) 55–60.
- B. Kok, B. Forbush, M. McGloin, Cooperation of charges in photosynthetic oxygen evolution. I. A linear four step mechanism, *Photochem. Photobiol.* 11 (1970) 457–475.
- P. Joliot, Period-four oscillations of the flash-induced oxygen formation in photosynthesis, *Photosynth. Res.* 76 (2003) 65–72.
- C.F. Yocum, The calcium and chloride requirement of the O_2 evolving complex, *Coord. Chem. Rev.* 252 (2008) 296–305.
- R.J. Debus, The manganese and calcium ions of photosynthetic oxygen evolution, *Biochim. Biophys. Acta* 1102 (1992) 269–352.
- A. Boussac, J.-L. Zimmermann, A.W. Rutherford, J. Lavergne, Histidine oxidation in the oxygen-evolving photosystem II enzyme, *Nature* 347 (1990) 303–306.
- X.-S. Tang, D.W. Randall, D.A. Force, B.A. Diner, R.D. Britt, Manganese-tyrosine interaction in the Photosystem II oxygen-evolving complex, *J. Am. Chem. Soc.* 118 (1996) 7638–7639.
- D.F. Ghanotakis, G.T. Babcock, C.F. Yocum, Calcium reconstitutes high rates of oxygen evolution in polypeptide depleted Photosystem II preparations, *FEBS Lett.* 167 (1984) 127–130.
- A. Boussac, A.W. Rutherford, Nature of the inhibition of the oxygen-evolving enzyme of Photosystem II induced by NaCl washing and revealed by the addition of Ca^{2+} or Sr^{2+} , *Biochemistry* 27 (1988) 3476–3483.
- C.-I. Lee, K.V. Lakshmi, G.W. Brudvig, Probing the functional of Ca^{2+} in the oxygen-evolving complex of photosystem II by metal ion inhibition, *Biochemistry* 46 (2007) 3211–3233.
- R. Pokhrel, I.L. McConnell, G.W. Brudvig, Chloride regulation of enzyme turnover: application to the role of chloride in photosystem II, *Biochemistry* 50 (2011) 2725–2734.
- J.W. Murray, K. Maghlaoui, J. Kargul, N. Ishida, T.-L. Lai, A.W. Rutherford, M. Sugiura, A. Boussac, J. Barber, X-ray crystallography identifies two chloride binding sites in the oxygen evolving centre of Photosystem II, *Energy Environ. Sci.* 1 (2008) 161–166.
- K. Kawakami, Y. Umena, N. Kamiya, J.-R. Shen, Location of chloride and its possible functions in oxygen-evolving photosystem II revealed by X-ray crystallography, *Proc. Natl. Acad. Sci. U. S. A.* 106 (2009) 8567–8572.
- A. Boussac, N. Ishida, M. Sugiura, F. Rappaport, Probing the role of chloride in Photosystem II from *Thermosynechococcus elongatus* by exchanging chloride for iodide, *Biochim. Biophys. Acta* 1817 (2012) 802–810.
- H. Wincencjus, C.F. Yocum, H.J. van Gorkom, Activating anions that replace Cl^- in the O_2 -evolving complex of photosystem II slow the kinetics of the terminal step

- in water oxidation and destabilize the S_2 and S_3 states, *Biochemistry* 38 (1999) 3719–3725.
- [16] P.M. Kelley, S. Izawa, The role of chloride ion in Photosystem II: I. Effects of chloride ion on Photosystem II electron transport and on hydroxylamine inhibition, *Biochim. Biophys. Acta* 502 (1978) 198–210.
- [17] N. Ishida, M. Sugiura, F. Rappaport, T.-L. Lai, A.W. Rutherford, A. Boussac, Biosynthetic exchange of bromide for calcium in the photosystem II oxygen-evolving enzymes, *J. Biol. Chem.* 283 (2008) 13330–13340.
- [18] A. Boussac, F. Rappaport, P. Carrier, J.-M. Verbavatz, R. Gobin, A. Kirilovsky, A.W. Rutherford, M. Sugiura, Biosynthetic Ca^{2+}/Sr^{2+} exchange in the photosystem II oxygen-evolving enzyme of *Thermosynechococcus elongatus*, *J. Biol. Chem.* 279 (2004) 22809–22819.
- [19] F. Rappaport, N. Ishida, M. Sugiura, A. Boussac, Ca^{2+} determines the entropy changes associated with the formation of transition states during water oxidation by Photosystem II, *Energy Environ. Sci.* 4 (2011) 2520–2524.
- [20] J. Kargul, K. Maghlaoui, J.W. Murray, Z. Deak, A. Boussac, A.W. Rutherford, I. Vass, J. Barber, Purification, crystallization and X-ray diffraction analyses of the *T. elongatus* PSII core dimer with strontium replacing calcium in the oxygen-evolving complex, *Biochim. Biophys. Acta* 1767 (2007) 404–413.
- [21] L.-E. Andréasson, I. Vass, S. Styring, Ca^{2+} depletion modifies the electron transfer on both donor and acceptor sides in Photosystem II from spinach, *Biochim. Biophys. Acta* 1230 (1995) 155–164.
- [22] J.L. Roose, L.K. Ranckel, T.M. Bricker, Documentation of significant electron transport defects on the reducing side of photosystem II upon removal of the PsbP and PsbQ extrinsic proteins, *Biochemistry* 49 (2010) 36–41.
- [23] A. Krieger, E. Weis, Energy-dependent of chlorophyll-*a*-fluorescence: the involvement of proton-calcium exchange at photosystem 2, *Photosynthetica* 27 (1992) 89–98.
- [24] A. Krieger, A.W. Rutherford, G.N. Johnson, On the determination of redox midpoint potential of the primary quinone electron acceptor, Q_A , in photosystem II, *Biochim. Biophys. Acta* 1229 (1995) 193–201.
- [25] A. Krieger, A.W. Rutherford, Comparison of chloride-depleted and calcium-depleted PSII: the midpoint potential of Q_A and susceptibility to photodamage, *Biochim. Biophys. Acta* 1319 (1997) 91–98.
- [26] T. Shibamoto, Y. Kato, M. Sugiura, T. Watanabe, Redox potential of the primary plastoquinone electron acceptor Q_A in photosystem II from *Thermosynechococcus elongatus* determined by spectroelectrochemistry, *Biochemistry* 48 (2009) 10682–10684.
- [27] T. Shibamoto, Y. Kato, R. Nagao, T. Yamazaki, T. Tomo, T. Watanabe, Species-dependence of the redox potential of the primary quinone electron acceptor Q_A in photosystem II verified by spectroelectrochemistry, *FEBS Lett.* 584 (2010) 1526–1530.
- [28] M. Sugiura, A. Boussac, T. Noguchi, F. Rappaport, Influence of Histidine-198 of the D1 subunit on the properties of the primary electron donor, P680, of photosystem II in *Thermosynechococcus elongatus*, *Biochim. Biophys. Acta* 1777 (2008) 331–342.
- [29] P. Mulo, C. Sicora, E.-M. Aro, Cyanobacterial psbA gene family: optimization of oxygenic photosynthesis, *Cell. Mol. Life Sci.* 66 (2009) 3697–3710.
- [30] Y. Nakamura, T. Kaneko, S. Sato, M. Ikeuchi, H. Katoh, S. Sasamoto, A. Watanabe, M. Iriguchi, K. Kawashima, T. Kimura, Y. Kishida, C. Kiyokawa, M. Kohara, M. Matsumoto, A. Matsuno, N. Nakazaki, S. Shimpō, M. Sugimoto, C. Takeuchi, M. Yamada, S. Tabata, Complete genome structure of the thermophilic cyanobacterium *Thermosynechococcus elongatus* BP-1, *DNA Res.* 9 (2002) 123–130.
- [31] P.B. Kós, Z. Deak, O. Cheregi, I. Vass, Differential regulation of *psbA* and *psbD* gene expression, and the role of the different D1 protein copies in the cyanobacterium *Thermosynechococcus elongatus* BP-1, *Biochim. Biophys. Acta* 1777 (2008) 74–83.
- [32] B. Loll, M. Broser, P.B. Kós, J. Kern, J. Biesiadka, I. Vass, W. Saenger, A. Zouni, Modeling of variant copies of subunit D1 in the structure of photosystem II from *Thermosynechococcus elongatus*, *Biol. Chem.* 389 (2008) 609–617.
- [33] J. Sander, M. Nowaczyk, J. Buchta, H. Dau, I. Vass, Z. Deák, M. Dorogi, M. Iwai, M. Rögner, Functional characterization and quantification of the alternative PsbA copies in *Thermosynechococcus elongatus* and their role in photoprotection, *J. Biol. Chem.* 285 (2010) 29851–29856.
- [34] C.I. Sicora, F.M. Ho, T. Salminen, S. Styring, E.-M. Aro, Transcription of a "silent" cyanobacterial *psbA* gene is induced by microaerobic conditions, *Biochim. Biophys. Acta* 1787 (2009) 105–112.
- [35] M. Sugiura, Y. Kato, R. Takahashi, H. Suzuki, T. Watanabe, T. Noguchi, F. Rappaport, A. Boussac, Energetics in photosystem II from *Thermosynechococcus elongatus* with a D1 protein encoded by either the *psbA1* or *psbA3* gene, *Biochim. Biophys. Acta* 1797 (2010) 1491–1499.
- [36] M. Sugiura, S. Ogami, M. Kusumi, S. Un, F. Rappaport, A. Boussac, Environment of TyrZ in Photosystem II from *Thermosynechococcus elongatus* in which PsbA2 is the D1 protein, *J. Biol. Chem.* 287 (2012) 13336–13347.
- [37] S. Ogami, A. Boussac, M. Sugiura, Deactivation processes in PsbA1-Photosystem II and PsbA3-Photosystem II under photoinhibitory conditions in the cyanobacterium *Thermosynechococcus elongatus*, *Biochim. Biophys. Acta* 1817 (2012) 1322–1330.
- [38] M. Sugiura, Y. Inoue, Highly purified thermo-stable oxygen-evolving photosystem II core complex from the thermophilic cyanobacterium *Synechococcus elongatus* having His-tagged CP43, *Plant Cell Physiol.* 40 (1999) 1219–1231.
- [39] A. Nakamura, T. Suzawa, T. Watanabe, Spectroelectrochemical determination of the redox potential of P700 in spinach with an optically transparent thin-layer electrode, *Chem. Lett.* 33 (2004) 688–689.
- [40] F. Comayras, C. Jungas, J. Lavergne, Functional consequences of the organization of the photosynthetic apparatus in *Rhodobacter sphaeroides*, *J. Biol. Chem.* 280 (2005) 11203–11213.
- [41] Y. Kato, M. Sugiura, A. Oda, T. Watanabe, Spectroelectrochemical determination of the redox potential of pheophytin a, the primary electron acceptor in photosystem II, *Proc. Natl. Acad. Sci. U. S. A.* 106 (2009) 17365–17370.
- [42] Y. Shibuya, R. Takahashi, T. Okubo, H. Suzuki, M. Sugiura, T. Noguchi, Hydrogen bond interactions of the pheophytin electron acceptor and its radical anion in photosystem II as revealed by Fourier transform infrared difference spectroscopy, *Biochemistry* 49 (2010) 493–501.
- [43] F. Rappaport, A. Cuni, L. Xiong, R. Sayre, J. Lavergne, Charge recombination and thermoluminescence in Photosystem II, *Biophys. J.* 88 (2005) 1948–1958.
- [44] F. Rappaport, J. Lavergne, Thermoluminescence: theory, *Photosynth. Res.* 101 (2009) 205–216.
- [45] L.B. Giorgi, P.J. Nixon, S.A.P. Merry, D.M. Joseph, J.R. Durrant, J.D.L. Rivas, J. Barber, G. Porter, D.R. Klug, Comparison of primary charge separation in the Photosystem II reaction center complex isolated from wild-type and D1-130 mutants of the cyanobacterium *Synechocystis* PCC 6803, *J. Biol. Chem.* 271 (1996) 2093–2101.
- [46] S.A.P. Merry, P.J. Nixon, L.M.C. Barter, M. Schilstra, G. Porter, J. Barber, J.R. Durrant, D.R. Klug, Modulation of quantum yield of primary radical pair formation in Photosystem II by site-directed mutagenesis affecting radical cations and anions, *Biochemistry* 37 (1998) 17439–17447.
- [47] K. Cser, I. Vass, Radiative and non-radiative charge recombination pathways in Photosystem II studied by thermoluminescence and chlorophyll fluorescence in the cyanobacterium *Synechocystis* 6803, *Biochim. Biophys. Acta* 1767 (2007) 233–243.
- [48] A. Boussac, M. Sugiura, T.-L. Lai, A.W. Rutherford, Low-temperature photochemistry in photosystem II from *Thermosynechococcus elongatus* induced by visible and near-infrared light, *Philos. Trans. R. Soc. B Biol Sci* 363 (2008) 1203–1210.
- [49] M.A. Strickler, L.M. Walker, W. Hillier, R.J. Debus, Evidence from biosynthetically incorporated strontium and FTIR difference spectroscopy that the C-terminus of the D1 polypeptide of photosystem II does not ligate calcium, *Biochemistry* 44 (2005) 8571–8577.
- [50] Y. Kimura, K. Hasegawa, T. Yamanari, T.-A. Ono, Studies on photosynthetic oxygen-evolving complex by means of Fourier transform infrared spectroscopy: calcium and chloride cofactors, *Photosynth. Res.* 84 (2005) 245–250.
- [51] H. Suzuki, Y. Taguchi, M. Sugiura, A. Boussac, T. Noguchi, Structural perturbation of the carboxylate ligands to the manganese cluster upon Ca^{2+}/Sr^{2+} exchange in the S-state cycle of photosynthetic oxygen evolution as studied by flash-induced FTIR difference spectroscopy, *Biochemistry* 45 (2006) 13454–13464.
- [52] R.M. Cinco, J.H. Robblee, J. Messinger, C. Fernandez, K.L.M. Holman, K. Sauer, V.K. Yachandra, Orientation of calcium in the Mn_4Ca cluster of the oxygen-evolving complex determined using polarized strontium EXAFS of photosystem II membranes, *Biochemistry* 43 (2004) 13271–13282.
- [53] Y. Pushkar, J. Yano, K. Sauer, A. Boussac, V.K. Yachandra, Structural changes in the Mn_4Ca cluster and the mechanism of photosynthetic water splitting, *Proc. Natl. Acad. Sci. U. S. A.* 105 (2008) 1879–1884.
- [54] H.H. Robinson, A.R. Crofts, Kinetics of the oxidation-reductions of the photosystem II quinone acceptor complex, and the pathway for deactivation, *FEBS Lett.* 153 (1983) 221–226.
- [55] S. Demeter, I. Vass, É. Hideg, A. Sallai, Comparative thermoluminescence study of triazine-resistant and -susceptible biotypes of *Erigeron canadensis* L., *Biochim. Biophys. Acta* 806 (1985) 16–24.
- [56] F. Rappaport, B.A. Diner, Primary photochemistry and energetics leading to the oxidation of the $(Mn)_4Ca$ cluster and to the evolution of molecular oxygen in Photosystem II, *Coord. Chem. Rev.* 252 (2008) 259–272.
- [57] R. Takahashi, K. Hasegawa, A. Takano, T. Noguchi, Structures and binding sites of phenolic herbicides in the Q_B pocket of photosystem II, *Biochemistry* 49 (2010) 5445–5454.
- [58] A. Boussac, M. Sugiura, F. Rappaport, Probing the quinone binding site of photosystem II from *Thermosynechococcus elongatus* containing either PsbA1 or PsbA3 as the D1 protein through the binding characteristics of herbicides, *Biochim. Biophys. Acta* 1807 (2011) 119–129.
- [59] I. Vass, K. Cser, Janus-faced charge recombinations in photosystem II photoinhibition, *Trends Plant Sci.* 14 (2009) 200–205.
- [60] A. Krieger-Liszczay, C. Fufezan, A. Trebst, Singlet oxygen production in photosystem II and related protection mechanism, *Photosynth. Res.* 98 (2008) 551–564.
- [61] A.W. Rutherford, A. Osyczka, F. Rappaport, Back-reactions, short-circuits, leaks and other energy wasteful reactions in biological electron transfer: redox tuning to survive life in O_2 , *FEBS Lett.* 586 (2012) 603–616.
- [62] A. Cuni, L. Xiong, R.T. Sayre, F. Rappaport, J. Lavergne, Modification of the pheophytin midpoint potential in Photosystem II: modulation of the quantum yield of charge separation and of charge recombination pathways, *Phys. Chem. Chem. Phys.* 6 (2004) 4825–4831.
- [63] B.R. Velthuis, Electron-dependent competition between plastoquinone and inhibitors for binding to photosystem II, *FEBS Lett.* 126 (1981) 277–281.
- [64] J. Lavergne, Mode of action of 3-(3, 4-dichlorophenyl)-1,1-dimethylurea: evidence that the inhibitor competes with plastoquinone for binding to a common site on the acceptor side of Photosystem-II, *Biochim. Biophys. Acta* 682 (1982) 345–353.